Original scientific paper

Effect of Fe, Ni, and Cr on the corrosion behaviour of hyper-eutectic Al-Si automotive alloy under different pH conditions

Mohammad Salim Kaiser[1,✉], Maglub Al Nur[2]

[1]*Directorate of Advisory, Extension and Research Services, Bangladesh University of Engineering and Technology, Dhaka-1000, Bangladesh*
[2]*Department of Mechanical Engineering, Bangladesh University of Engineering and Technology, Dhaka-1000, Bangladesh*

Corresponding author - E-mail:[✉]mskaiser@iat.buet.ac.bd; Tel.: +88-9663129; Fax: +88-9665622

Abstract

Effect of Fe, Ni and Cr on the corrosion behaviour of hyper-eutectic Al-Si automotive alloy was studied. The test of corrosion behaviour at different environmental pH 1, 3, 5, 7, 9, 11 and 13 was performed using conventional gravimetric measurements and complemented by resistivity, optical micrograph, scanning electron microscopy (SEM) and X-ray analyser (EDX) investigations. The highest corrosion rate was observed at pH 13 followed by pH 1, while in the pH range of 3.0 to 11, there is a high protection of surface due to formation of stable surface oxide film. The highest corrosion rate at pH 13 is due to presence of sodium hydroxide in the solution in which the surface oxide film is soluble. At pH 1, however, high corrosion rate can be attributed to dissolution of Al due to the surface attack by aggressive chloride ions. Presence of Fe, Ni and Cr in hyper-eutectic Al-Si automotive alloy has significant effect on the corrosion rate at both environmental pH values. Resistivity of alloy surfaces initially decreases at pH 1 and pH 13 due to formation of thin films. The SEM images of corroded samples immersed in pH 1 solution clearly show pores due to uniform degradation of the alloy. In pH 13 solution, however, the corrosion layer looks more packed and impermeable.

Keywords
Al-Si alloy; alloying elements; environmental pH; corrosion; gravimetric analysis; surface resistivity; SEM

Introduction

Al–Si alloys with more than 13 % of silicon content are termed as hyper-eutectic alloys. These types of alloys are used for building up cylinder blocks, pistons and valve filters, *etc.* In recent years, the understanding of eutectic solidification in Al-Si based casting alloys has attracted a great

attention of many researchers [1-3]. A number of researchers have investigated the role of added alloying elements, like Mg, Cu, Mn, Ni, Zn, Fe, Ni, Cr and Pb, on the microstructural and mechanical performances of Al-Si alloys [4-6]. It has been found that even small content of iron increases strength and fluidity, while higher iron concentration increases hardness and supports segregation of brittle and hard intermetallic phases. Presence of Ni in aluminium alloys generally provides additional strengthening by forming various nickel aluminide precipitates [7]. Small amount of added Cr has shown a significant effect in refining the grain size of Al-Si-Mg alloys. Presence of Cr moderately improves the mechanical properties such as yield strength, ultimate tensile strength and fracture toughness [8]. Alloying elements that are added to achieve certain mechanical properties change the corrosion behaviour of the alloys, where important factors are the types and concentrations of the added elements, *e.g.* whether they are present in solid solution or as intermetallic particles. However, very limited work has been carried out on the influence of added alloying elements Fe, Ni, Cr and clarification of their role on the corrosion behaviour of Al-Si alloy.

Corrosion is a natural process of slow degradation of metals or metal alloys, created by the electrochemical reaction with the surrounding environment. Rate of corrosion depends on their chemical composition and the aggressiveness of the environment. Since the Al-Si hypereutectic alloy should work in different atmosphere of different pH, the purpose of the present study is to find out the effect of added Fe, Ni and Cr on its corrosion characteristics under different environmental pH conditions.

Experimental

Aluminium engine block was melted in a resistance furnace under the suitable flux cover (degasser, borax etc.) which was used as the master alloy. Four alloys were casting for developing hyper-eutectic Al-Si automotive alloy. Alloy 1 was prepared by re-melting the master alloy. Then mild steel chips were added with the master alloy in order to prepare Alloy 2 (Fe added). Alloy 3 (Fe and Ni added) was prepared by adding mild steel chips and Ni with master alloy. Some stainless-steel chips, containing large amounts of Ni and Cr, were added with the master alloy to prepare Alloy 4 (Fe, Ni and Cr added). The final temperature of the melt was always maintained at 750±15 °C. Casting was done in cast iron metal moulds preheated to 200 °C. Mould sizes were 16×150×300 mm. The alloys were analysed simultaneously, by using wet chemical and spectrochemical methods. The chemical compositions of alloys are given in Table 1. The cast alloy was homogenized in a Muffle furnace at 400 °C for 18 hours and air cooled to relieve internal stresses and for homogenization. The homogenized samples were solutionized at 530 °C for 2 hours, followed by the salt ice water quenching to get a super saturated single phase. The obtained samples of 55×15×3 mm size was artificially aged at 175 °C for 240 minutes and then the tests for studying the corrosion behaviour were conducted.

Table 1. Chemical composition of experimental Al-Si alloys.

	Content, wt%									
	Si	Fe	Ni	Cr	Cu	Mg	Zn	Mn	Ti	Al
Alloy 1	19.209	0.795	0.089	0.040	2.826	0.245	1.117	0.214	0.099	Bal
Alloy 2	17.947	5.910	0.091	0.086	2.881	0.186	1.139	0.183	0.071	Bal
Alloy 3	18.913	6.256	0.567	0.057	2.889	0.193	1.124	0.178	0.090	Bal
Alloy 4	19.363	5.501	0.621	1.267	3.112	0.232	1.085	0.217	0.076	Bal

Hardness of the aged alloys was measured in the Vickers hardness testing machine at 2 kg load and an average of ten concordant readings was taken as the representative hardness of the sample. The samples were wet-sanded mechanically with SiC papers of 220 and 1200 grit. Before use, the samples were de-greased with ethanol of 99 % purity and then rinsed with plenty of water. After-wards, they were dried, weighted (initial weight, W_{int}) and immersed in corrosive media for different exposure periods up to 27 days. Stagnant solutions of different pH were used as corrosive media. Solutions of pH 1, pH 3 and pH 5 were prepared by adding 20, 0.2 and 0.002 mL of 10 mol dm^{-3} HCl into 2000 mL of distilled water. Solutions of pH 9, pH 11 and pH 13 were prepared by adding 0.02, 2 and 200 mL of 1 mol dm^{-3} NaOH into 2000 mL of distilled water. Pure distilled water was used as the pH 7 solution. All solutions were prepared and used at room temperature. After expiring of a designated exposure time in the solution medium, the samples were rinsed with distilled water, dried between two tissue papers and weighted again (final weight, W_{fin}). Weight-loss measurements were made in triplicate and each weight loss was calculated by taking the average of these values. The weight loss and the corrosion rate over the exposure time period were calculated according to the following relations [9]:

$$\Delta W = \frac{W_{int} - W_{fin}}{A} \qquad (1)$$

$$K_{Corr} = \frac{K \Delta W}{TD} \qquad (2)$$

ΔW = weight loss, mg/cm^2

W_{int} = initial weight before immersion, mg

W_{fin} = final weight after exposure, mg

A = area, cm^2

K_{Corr} = corrosion rate, mm/year

K = unit conversion constant (87.6 for the mm/year unit)

T = time of exposure, h

D = density of metal, g/cm^3

Electrical conductivity measurements of the alloy surfaces in different conditions were carried out with an Electric Conductivity Meter, type 979. Electrical resistivity was calculated from the electrical conductivity data. The specimens for microstructural observation were prepared using standard metallographic techniques. The final polishing was done with fine alumina, while etching was done using Keller's reagent (HNO$_3$ + 2.5 cm^3, HCl + 1.5 cm^3, HF + 1.0 cm^3 and H$_2$O + 95.0 cm^3). The washed and dried samples were observed by OPTIKA Microscope and some selected photomicrographs were taken. The SEM investigation and EDX analysis were obtained for the surface of the alloys specimens after their immersion in solution media for 27 days. The SEM images were collected using a JEOL scanning electron microscope with an energy dispersive X-ray analyzer (Model: Link AN - 10000) attached.

Results and discussion

Hardness

Figure 1 shows hardness of hyper-eutectic Al-Si automotive Alloy 1, Alloy 2 (Fe added), Alloy 3 (Fe and Ni added), and Alloy 4 (Fe, Ni and Cr added), all being artificially aged at 175 °C for 240 minutes. It is observed in Figure 1 that all alloys attainted higher hardness than the base Alloy 1. This is due to higher amount of Fe in the alloys, resulting in formation of variety of Fe-rich inter-

metallic phases such as Al_3Fe, α-Al_8Fe_2Si, β-Al_5FeSi, δ-Al_4FeSi_2 and γ-Al_3FeSi. Among these phases, the β-Al_5FeSi phase was found especially hard [10]. Slightly higher hardness of the Alloy 3 is due to the precipitation hardening effect in the presence of Al_3Ni intermediate phase in to the Al matrix [11]. The Alloy 4 losses small amount of the hardness, because Cr modified morphology and type of Fe-rich intermetallic phase and suppressed formation of hard β-Al_5FeSi phase in the alloys [12].

Figure 1. *Variation of Vickers hardness of different Al-Si alloys artificially aged at 175 °C for 240 minutes*

Gravimetric analysis

The weight losses, ΔW, after immersion of 3 days were calculated using Eq. (1) for the hypereutectic Al-Si automotive Alloys 1–4 and as a function of the environmental pH presented in Fig. 2.
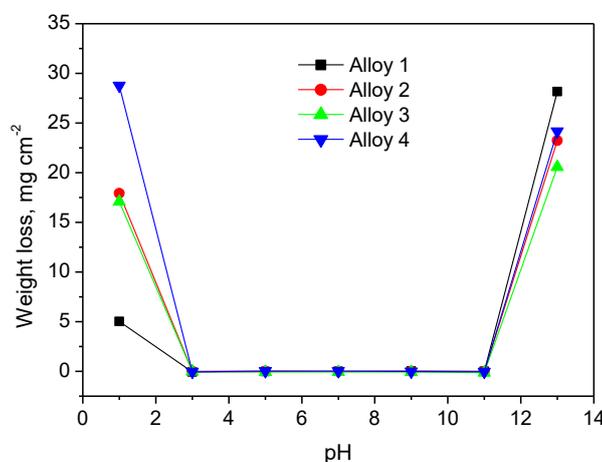

Figure 2. *Variation of the weight loss as a function of environmental pH*

Figure 2 shows that the weight loss of the alloys is the lowest in the pH range of 3 to 11, while at pH 1 and pH 13, the weight loss becomes higher. At pH 1, the oxygen reacts with absorbed atomic hydrogen, thereby depolarizing the surface and allowing the partial cathodic reaction to continue together with anodic dissolution of Al. The presence of such surfaces can be attributed to the dissolution of Al due to the surface attack by the aggressive chloride ions. At pH 13, a partial anodic reaction is aluminium dissolution proceeding through hydroxide film formation and its concomitant dissolution. It seems that aggression of NaOH on the aluminium alloy is higher than HCl, what is clear after comparison of weight losses in two solutions. Typically, the corrosion rate of aluminium increases exponentially for pH values lower than $\sim$3 or higher than $\sim$9 [13].

In the pH range of ~4 to 9, Al is nominally passive due to the presence of Al_2O_3 film on its surface. In environments that deviate from a near neutral range, the continuity of this film can be disrupted, making the film soluble and facilitating relatively rapid dissolution of the alloy. In the acidic range, Al is oxidized by forming Al^{3+} ions, whilst formation of AlO_2^- ions occurs in the alkaline range [14]. Plots of the corrosion rates, K_{Corr}, calculated from the weight loss tests using Eq. (2), are presented in Figures 3 and 4 for all experimental Al-Si alloys exposed during 27 days in pH 1 and pH 13 solutions. Both figures show normal corrosion profiles, characteristic for most passivating metals including Al, subjected to corrosive environments. Corrosion profile of each alloy shows the initial steep rise in corrosion rate, until a peak value is reached, corresponding to the active dissolution region. After that, the corrosion rate progressively declines because of passivity which is due to adherence of the oxides formed on the metal surface.
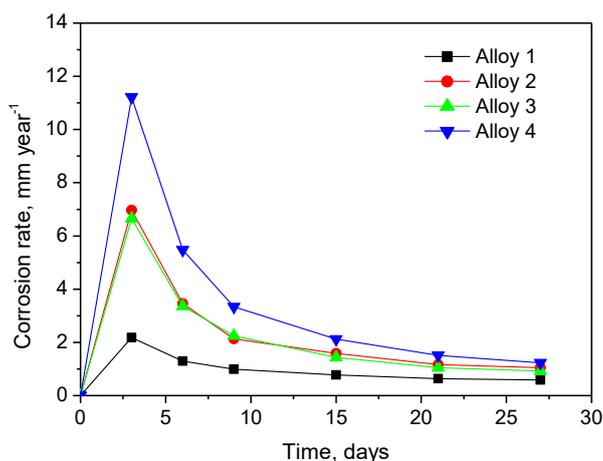

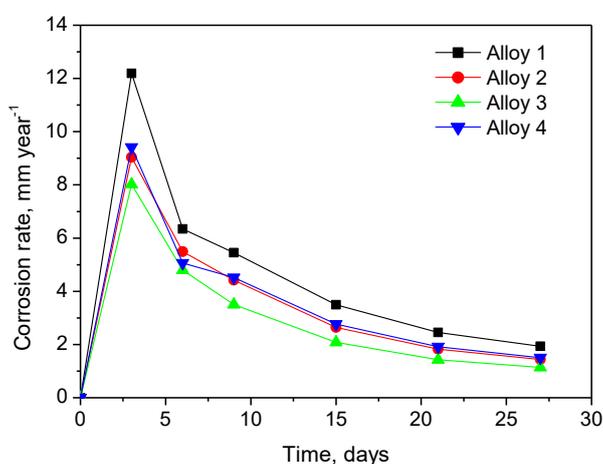**Figure 3.** *Change of corrosion rate of Al-Si alloys as a function of immersion time at pH 1*

Figure 4. *Change of corrosion rate of Al-Si alloys as a function of immersion time at pH 13*

The highest corrosion rate at pH 13 is due to presence of sodium hydroxide in the solution in which the surface oxide film is soluble and aluminium dissolves uniformly at a steady rate. When pH is decreasing (acidity increases), the corrosion rate is also increased. This is because low pH solutions accelerate corrosion by providing hydrogen ions, what raised the redox potential with a consequent increase in the reaction rate. Also, chloride ions affect the corrosion behaviour of the alloy in acidic solutions in a sense that increase of chloride ions increased the corrosion rate [15]. It can be seen in Figures 3 and 4 that for each alloy, K_{Corr} values initially increased quite abruptly until immersion time of 3 days and afterwards attained roughly constant values with immersion time. At higher time

periods of exposure, accumulation of corrosion products (including aluminium oxide and hydroxide) covering up the surface led to decreased and uniform weight loss caused by the constant corrosion rate. Although aluminium is a reactive metal, it shows a very good corrosion resistance because of a thin surface layer of aluminium oxide formed in the air which prevents further corrosion. This film is quite stable in neutral and mildly acidic solutions, but dissolves more readily in the alkaline pH range. This is supported by the results for the Alloy 1 presented in Figures 3 and 4 that show the lowest K_{Corr} at pH 1 and the highest K_{Corr} at pH 13.

Figure 3 also suggests that at the environmental pH 1, presence of the iron in the Al-Si alloy is detrimental, since K_{Corr} was increased for all Fe added alloys (Alloys 2−4). This is due to its low solubility and hence ability to form constituent particles such as Al_3Fe, which are cathodic as hydrogen ions are plentiful to the Al matrix. Additionally, iron can sustain chemical reactions more efficiently than Al [16]. In more complex alloys, Fe can also combine with other alloying elements such as Ni (Alloy 3), which is also a major issue for corrosion since the combination of Fe and Ni provides its greater efficiency [17]. Transition metals such as Cr are usually not employed owing to their very low solubility limits, what is supported with the highest K_{Corr}, observed for the Alloy 4 in Figure 3. Figure 4 shows that at pH 13 solution, all Fe, Ni and Cr added alloys (Alloys 2−4), exhibited lower corrosion rates than Alloy 1. This is in accordance with Shaw *et al.* [18], who successfully produced the alloys by sputter deposition and found that these elements increased the pitting potential and passivity of the alloys.

As obvious in Figures 5 and 6, when the alloys are immersed for 27 days in pH 1 and pH 13 solutions, the resistivity values of the surfaces showed a general decreasing trend within the first few days of immersion. This is since each alloy surface reacts with oxygen molecules and forms a very thin film of aluminium oxide and hydroxide which decreases the resistivity [19]. For prolonged exposure time at low pH, a continuous degradation of the alloys produced pits and formation of uneven surface which increases the electrical resistivity of the surface of all experimental alloys. A bond of thin film to its surface reduces the resistivity. Pit formations seen through resistivity increase for the Alloy 2 (Fe added), Alloy 3 (Fe and Ni added) and Alloy 4 (Fe, Ni and Cr added) are more prominent with respect to the base Alloy 1 (Fig. 5).
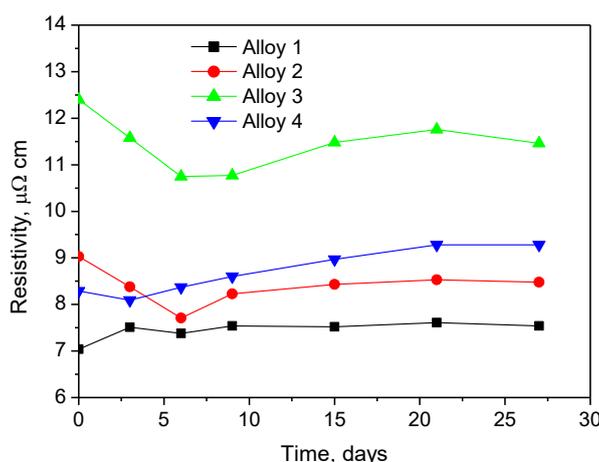

Figure 5. *Change of resistivity of Al-Si alloys as a function of immersion time at pH 1*

This has also been shown above with the corrosion rate profile at the environmental pH 1. At pH 13, aluminium forms a very thin film of aluminium oxide and hydroxide, having a bond to its surface which reduces the resistivity. After prolonged exposure time, the thickness of thin film

increases and produces the surface cracking which caused increased resistivity of the alloys (Fig. 6). The rate of formation of thin film is lower for the Alloy 1 with respect to other alloys and this agrees with the corrosion rate profile in pH 13 solution. The initial resistivity of the alloys is different because of the presence of a variety of elements in the alloys.
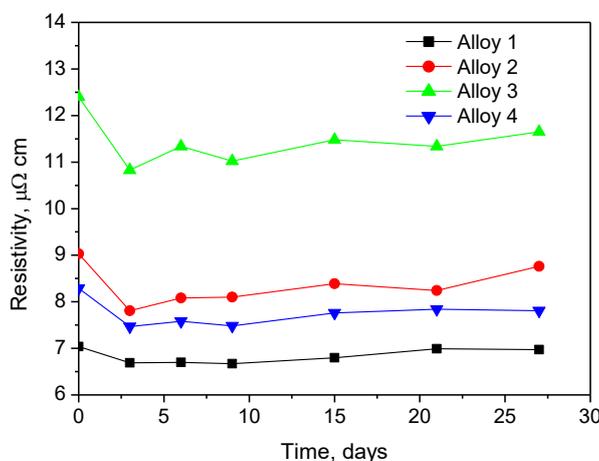

Figure 6. *Change of resistivity of Al-Si alloys as a function of immersion time at pH 13*

Optical micrographic observation

Figure 7 shows the optical micrographs of polished Al-Si alloys taken before and after immersion for 3 days in solutions of different pH. The samples before corrosion show a microstructure with distinguished α- matrix, eutectic Si particles in α-matrix and many Cu- and Fe-rich intermetallic phases. These types of microstructure show two tones, where darker tone is associated with precipitates of Al (Mn, Fe, Cu) and lighter tone is due to Al (Si, Mg) precipitates. The intensity of two tones is different for different alloys due to presence of different alloying elements in the alloys [20]. Some scatters are observed owing to the polishing.

It is also seen in Figure 7 that after removing samples from solutions of different pH to which they were exposed at room temperature for 3 days, a severe corrosion was observed. These findings primarily suggested that low pH 1 and high pH 13 solutions are very aggressive environmental media that induced high corrosion of the aluminium alloys. In the case of pH 1, the pit formation on the surface is prominent, what is due to the surface attack by the aggressive chloride ions [21]. The microstructure of corroded samples in pH 13 solution show degradation of alloy surfaces, providing more or less uniform attack of hydroxide ion on the surface of metal [15]. Some extent of corrosion observed at pH 7 solution can be explained by presence of some free hydrogen ions in distilled water, and their multiplication by free carbon dioxide dissolved in the water. Carbon dioxide reacts with water by formation of the carbonic acid that is an effective source of acidity.

Figure 8 illustrates the optical microstructures of hyper-eutectic Al-Si automotive Alloys 1−4 aged at 175°C for 4 hours. Structure of the Alloy 1 consists of α-phase, eutectic Si, primary Si particles and intermetallic phases (Fig. 8a). The primary Si exhibited the blocky morphology, while the eutectic silicon exhibited needle shape morphology [19]. Alloy 2 is composed of eutectic structure α-Al and Si in which the coarse intermetallic phases Al_5FeSi and Al_2FeSi are dispersed (Fig. 8b). Alloy 3 shows that nickel stabilizes different types of Al-Fe-Si phase formed in the alloy (Fig. 8c) [22]. Addition of Cr in the Alloy 4 resulted in a finer microstructure (Fig. 8d). This is probably caused by the ability of Cr to modify the morphology of the commonly observed β-Al_5FeSi phases into the more beneficial α-$Al_{15}(Fe,Mn,Cr)_3Si_2$ intermetallic phases while the content of Si remained the same [23].
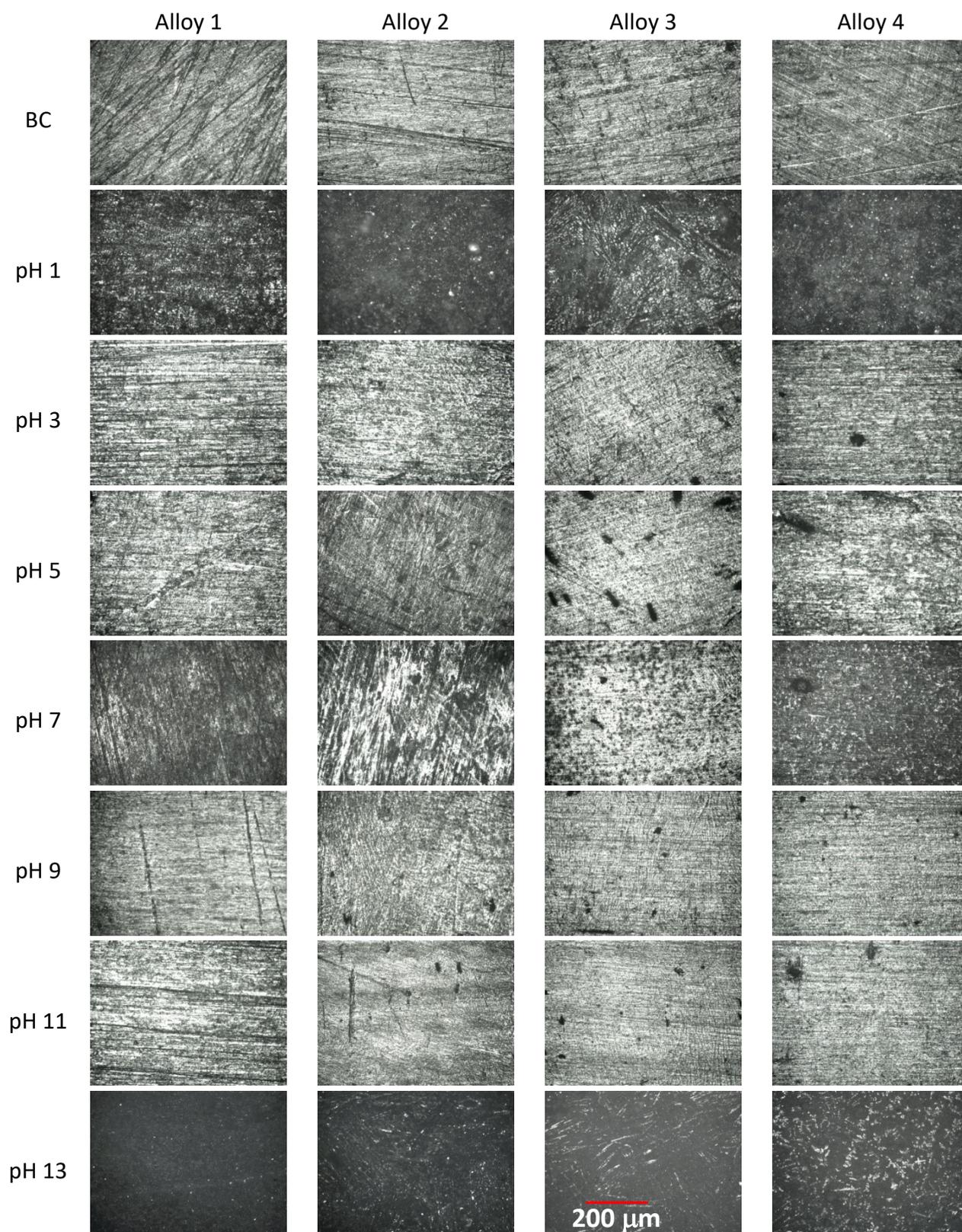
Figure 7. *Microstructure of polished Al-Si alloys before (BC) and after corrosion at different environmental pH for 3 days*
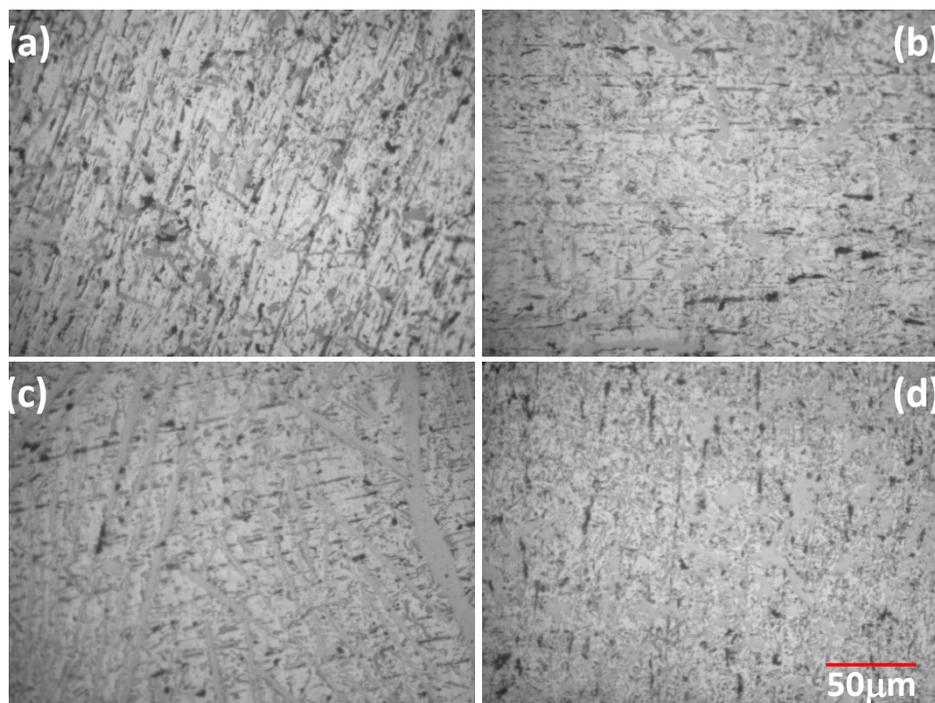
Figure 8. *Microstructure of Al-Si alloys aged at 175°C for 240 minutes:*
(a) Alloy 1, (b) Alloy 2, (c) Alloy 3 and (d) Alloy 4

SEM and EDX observation

SEM images of samples corroded in pH 1 medium after 27 days of immersion are presented in Figure 9. All images clearly show spherical, narrow and superficial pits dispersed on the surfaces of alloys. The crystallographic cubic shaped pitting is characteristic of corrosion in chlorides and is due to the uniform degradation of alloys. High aggressive attack of chloride ions breaks down the passive film formed on the surface of the alloys [15]. The nature and intensity of pitting are dissimilar for the alloys because of the presence of different amounts of intermetallics in the alloys. Content of the elements by weight of the Alloy 1, found by the corresponding EDX analysis of the SEM (Fig. 9a), are: 51.21 % O, 0.04 % Na, 21.84 % Al, 11.82 % Si, 1.21 % S, 0.27 % Cl, 0.20 % Ti, 0.30 % Cr, 0.43 % Fe, 0.87 % Cu, 11.83 % Br. Content of the elements by weight of the Alloy 2 Fig. 9b) are: 59.44 % O, 0.05 % Mg, 17.38 % Al, 1.0 % Si, 1.29 % S, 1.96 % Cl, 0.72 % Fe, 0.11 % Ni, 0.41 % Cu, 17.39% Br and 0.25% Zr. For the Alloy 3, content of the elements by weight (Fig. 9c) are: 60.15 % O, 18.72 % Al, 3.18 % Si, 1.35 % S, 0.12 % Cl, 0.51 % Ti, 0.16 % Cr, 0.70 % Fe, 0.32 % Ni, 0.36 % Cu and 14.06 % Br. For the Alloy 4 (Fig. 9d), content of the elements by weight are: 56.92 % O, 17.23 % Al, 4.35 % Si, 1.33 % S, 0.60 % Cl, 0.83 % Cr, 1.28 % Fe, 0.01 % Ni, 2.03 % Cu and 15.41 % Br. Lower percents of oxide found for the Alloy 1 (51 %) compared to other alloys (57-60 %) indicates lower amount of degradation, what is in agreement with the lowest corrosion rate of this alloy discussed earlier with Figure 3.

SEM images of corroded samples after corrosion tests performed in pH 13 medium after 27 days of exposure are shown in Figure 10. For samples immersed in pH 13 solution, a black corrosion product layer was formed on the surface of the alloys during the corrosion process, and this layer became thicker at higher NaOH concentrations. In alkaline solution, the corrosion layer seems more compact, homogenous and not porous [19]. Content of the elements by weight of the Alloy 1 found by EDX analysis of the SEM (Fig. 10a) at pH 13 solution are: 50.58 % O, 8.99 % Na, 1.22 % Mg, 11.38 % Al, 13.98 % Si, 0.09 % S, 0.05 % Cl, 0.03 % Ti, 0.55 % Cr, 1.03 % Fe, 1.89 % Ni, 2.02 % Cu, 8.01 % Br and 0.25 % Zr.
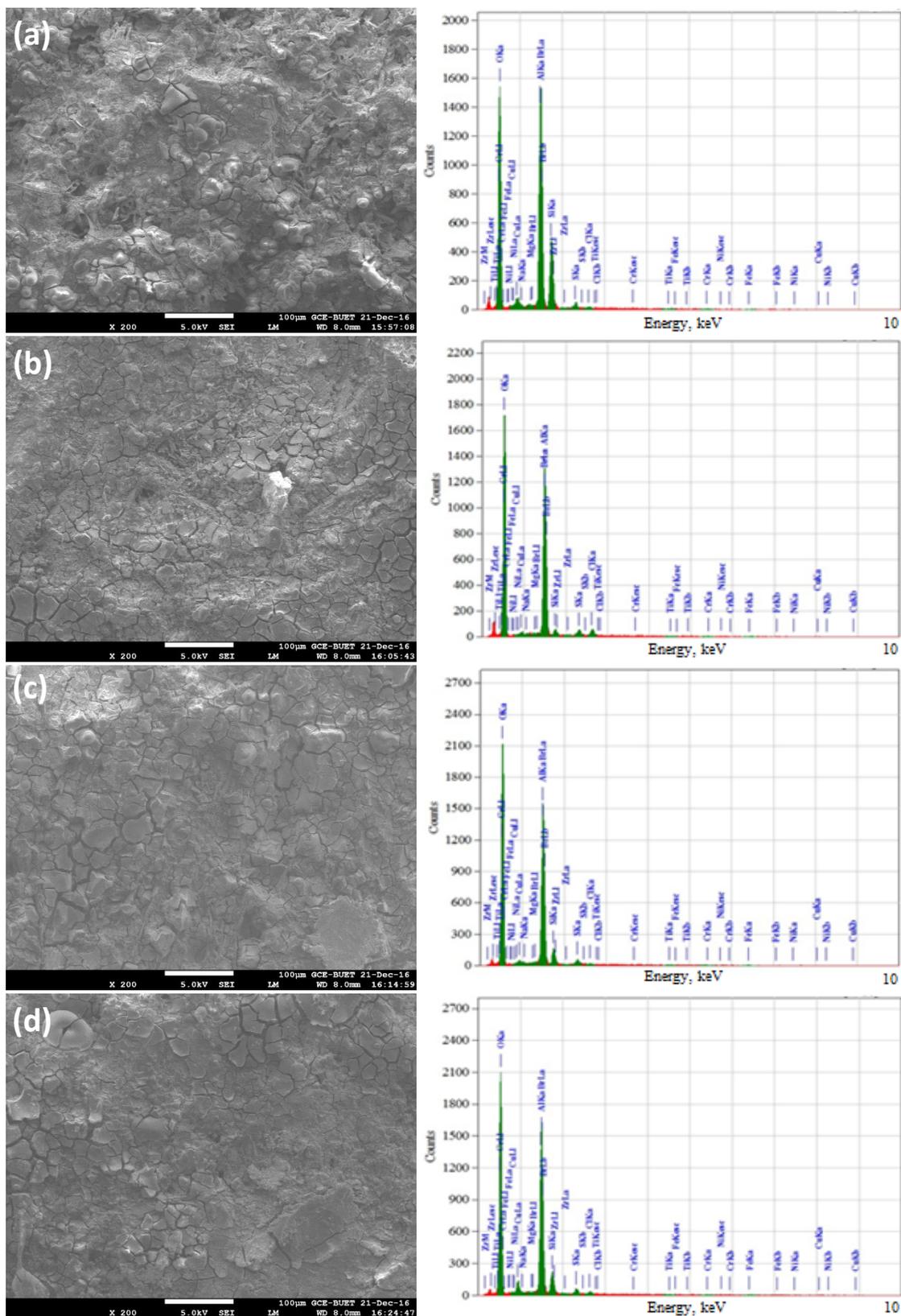
Figure 9. *SEM images and EDX spectra of Al-Si alloys after exposure in pH 1 solution for 27 days:*
(a) *Alloy 1,* ***(b)*** *Alloy 2,* ***(c)*** *Alloy 3 and* ***(d)*** *Alloy 4*

Content of the elements by weight of Alloy 2 (Fig. 10b) at pH 13 solution are: 46.92 % O, 5.85 % Na, 0.83 % Mg, 15.28 % Al, 12.23 % Si, 0.05 % S, 0.10 % Cl, 0.14 % Ti, 2.70 % Fe, 1.29 % Ni, 1.88 % Cu, 12.69 % Br and 0.02 % Zr.
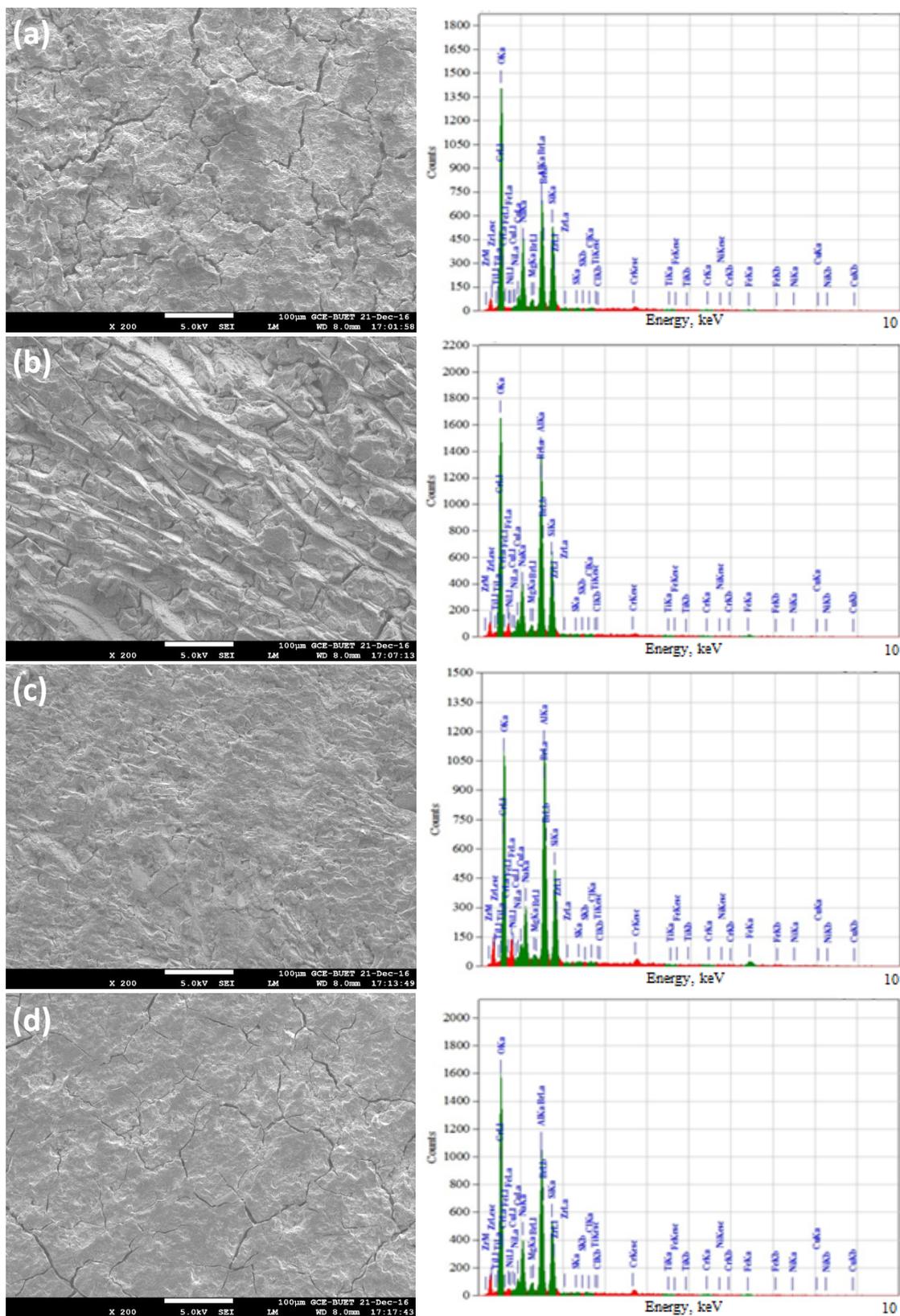
Figure 10. *SEM images and EDX spectra of Al-Si alloys after exposure in pH 13 solution for 27 days:*
(a) Alloy 1, (b) Alloy 2, (c) Alloy 3 and (d) Alloy 4

Similarly, for Alloy 3 (Fig. 10c), content of the elements by weight are: 37.90 % O, 5.64 % Na, 0.50 % Mg, 13.84 % Al, 11.17 % Si, 0.19 % S, 0.15 % Cl, 0.28 % Cr, 10.75 % Fe, 2.15 % Ni, 2.05 % Cu, 15.09 % Br and 0.14 % Zr. For Alloy 4 (Fig. 10d) at pH 13 solution, content of the elements by weight are: 48.40 % O, 6.43 % Na, 1.25 % Mg, 11.37 % Al, 11.47 % Si, 0.07 % S, 0.94 % Cr, 2.66 % Fe, 0.77 %

Ni, 1.47 % Cu, 14.96 % Br and 0.21 % Zr. It is noted from the EDX data that the percentage of oxygen indicates the corrosion of the alloys. Higher corrosion means higher dissolution of Al and higher corrosion rate as discussed earlier with Figure 4. Also, presence of oxygen originated from the formation of aluminium oxide layer on the surface of the alloy, which in turn leads to decreasing the corrosion of the alloy. In case of pH 13 the sodium oxide is visible on the surface of the alloy.

Conclusions

From the results obtained, it can be concluded that higher corrosion rates of the hyper-eutectic Al-Si automotive alloy observed at both environmental pH 1 and pH 13 are due to the surface attack by the aggressive chloride ions and solubility of surface oxide film, respectively. Insertion of the alloying elements Fe, Ni and Cr increased the corrosion rate of the Al-Si alloy at the environmental pH 1 but decreased the corrosion rate at the environmental pH 13. At the same time, a stable oxide film formed on the surfaces of all alloys protected them from corrosion in the pH range of 3.0 to 11. Decreased resistivity values of the alloys in corrosive solutions of pH 1 and pH 13 were due to formation of thin films of oxide and hydroxide. Corroded samples immersed in pH 1 solution clearly showed pores, what was due to the uniform degradation of the alloys. When immersed in pH 13 solution, a black corrosion product layer was formed on the surfaces of the alloys.

References

[1]   P. S. Mohanty, J. E. Gruzleski, *Acta Mater.* **44(9)** (1996) 3749-3760.
[2]   R. K. Singh, A. Telang , S. Das, *American Journal of Engineering Research* **5(8)** (2016) 133-137.
[3]   M. S. Kaiser, *International Journal of Materials Science and Engineering* **5(2)** (2017) 87-94.
[4]   M. N. E. Efzan, H. J. Kong, C. K. Kok, *Advanced Materials Research* **845** (2013) 355-359.
[5]   S. G. Shabestari, H. Moemeni, *Journal of Materials Processing Technology* **153–154** (2004) 193-198.
[6]   S. G Shabestari, *Materials Science and Engineering A* **383** (2004) 289-298.
[7]   R. S. Rana, R. Purohit, S. Das, *International Journal of Scientific and Research Publications* **2(6)** (2012) 1-7.
[8]   A. Kumar, G. Sharma, C. Sasikumar, S. Shamim, H. Singh, *Applied Mechanics and Materials* **789-790** (2015) 95-99.
[9]   H. H. Strehblow, *Corrosion Mechanism in theory and practice.* Marcel Dekker, New York, *(1995)*
[10]   X. Cao, J. Campbell, *Materials Transactions* **47(5)** (2006) 1303-1312.
[11]   S. A. Awe, S. Seifeddine, A. E. W. Jarfors, Y. C. Lee, A. K. Dahle, *Advanced Materials Letters* **8(6)** (2017) 695-701.
[12]   W. Eidhed, *Journal of Materials Science and Technology* **24(1)** (2008) 45-47.
[13]   S. Adhikari, *Alkaline dissolution of aluminium: surface chemistry and subsurface interfacial phenomena,*Ph.D thesis, Lowa State University, Ames, Lowa, USA, (2008)
[14]   M. Pourbaix, *Atlas of electrochemical equilibria in aqueous solutions*, 2nd edition, National Association of Corrosion Engineers, Houston, TX, USA.1974.
[15]   D. Prabhu, P. Rao, *Arabian Journal of Chemistry* **10(2)** (2017) 2234-2244.
[16]   J. R. Galvele, *Journal of the Electrochemical Society* **123(4)** (1976) 464-474.
[17]   N. Birbilis, M. K. Cavanaugh, R. G. Buchheit, *Corrosion Science* **48(12)** (2006) 4202-4215.
[18]   B. A. Shaw, T. L. Fritz, G. D. Davis, W. C. Moshier, *Journal of the Electrochemical Society* **137(4)** (1990) 1317-1318.
[19]   M. Al Nur, M. S. Kaiser, *International Journal of Mechanical and Materials Engineering* **11(11)** (2017) 1736-1740.

[20] M. S. Kaiser and S. Dutta, International Journal of Advances in Materials Science and Engineering **1(1)** (2014) 9-17.

[21] A. A. El Maghraby, *The Open Corrosion Journal* **3** (2010) 54-57.

[22] A. Skolakova, P. Novak, D. Vojtech, T. F. Kubatik, *Materials and Design* **107** (2016) 491-502.

[23] T. S. Kim, C. Suryanarayana, B. S. Chun, *Materials Science and Engineering* **278** (2000) 113–120.